Nuclear Winter Could Sever Urban Water Access Across the Northern Hemisphere

Juan Esteban Lamilla Cuellar [a]* (iD), *Rachel Palm* [a] (iD), *David C. Denkenberger* [a,b] (iD), *Florian Ulrich Jehn* [a] (iD)

Affiliations:

[a] *Alliance to Feed the Earth in Disasters (ALLFED)*

[b] *University of Canterbury, Department of Mechanical Engineering*

* Corresponding author: juan_lamilla@allfed.info

Abstract

The continuous functioning of the underground water supply networks is essential for many aspects of modern civilization. Therefore, it is essential to keep such critical infrastructure safe from disasters. However, existing risk assessment studies often assume relatively stable climate conditions. Abrupt sunlight reduction scenarios, such as those caused by a nuclear war, a large volcanic eruption, or an asteroid impact, could cool the planet by up to 10°C and thus frost-damage water pipes. This study investigates such vulnerability of the global underground water supply network in urban areas, in a nuclear winter – one such abrupt climate shift resulting from a nuclear war. We use climate modeling data simulating a nuclear exchange between Russia and the United States of America, in combination with predictions of the network location and density derived from nighttime light and artificial impervious surface data. By considering an increase in maximum frost depth under nuclear winter conditions, we identify areas where such networks are most vulnerable to disruption, and predict the length of the potentially affected pipelines using population-size-based and street-network-length-based models. As estimated, a total of ~5–9 million kilometers of this critical infrastructure in 92 countries is at risk of freezing, potentially impacting the primary water source of over 2 billion individuals. Our findings highlight the need to expand the scope of climate resilience assessments in water risk research to include a broader range of climate scenarios, including sudden cold shifts.
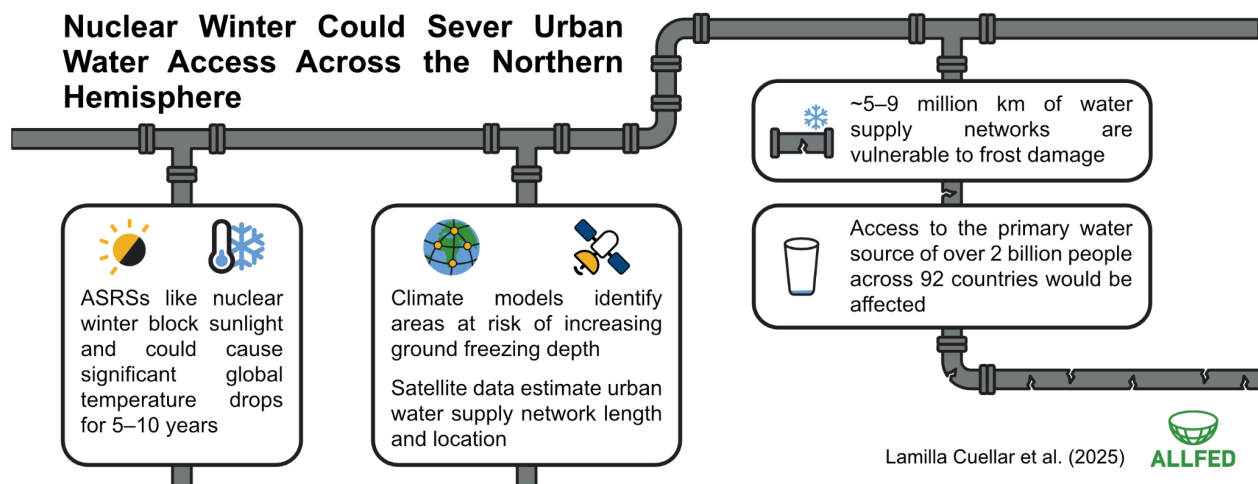
Keywords

Highlights

- In the nuclear winter scenario, maximum frost depth increases may affect 92 countries

- Only the Northern Hemisphere may be affected significantly

- Over 2.1 billion people may lose access to water due to frost damage to pipes

- More than 8.8 million km of underground water supply networks might be affected

- For pipeline length, street network length is a better predictor than population size

Graphical abstract

Nuclear Winter Could Sever Urban Water Access Across the Northern Hemisphere

~5–9 million km of water supply networks are vulnerable to frost damage

Access to the primary water source of over 2 billion people across 92 countries would be affected

ASRSs like nuclear winter block sunlight and could cause significant global temperature drops for 5–10 years

Climate models identify areas at risk of increasing ground freezing depth

Satellite data estimate urban water supply network length and location

Lamilla Cuellar et al. (2025)

ALLFED

Glossary

- *at-risk area* – area with an increase in maximum frost depth in the scenario

- *at-risk urban area* – at-risk area also identified as being urban; assumed to have an underground water supply network

- *pipeline* – underground water supply network (synonym)

- *urban area* – area identified as being urban; assumed to have an underground water supply network

1. Introduction

Water supply networks are essential systems underlying modern civilization. They are lifelines, enabling the continuous operation of critical government and business functions, essential to human health and safety or economic security (FEMA, 2024). As of 2022, such piped infrastructure had the potential to deliver safe water (WHO and UNICEF, 2021) to households with a total of ~5.3 billion individuals, ~3.8 billion of which were urban dwellers (WHO and UNICEF, n.d.). Piped water systems can provide dramatic health benefits such as decreased diarrhoeal disease mortality, improved welfare, mental well-being, and social health, alongside advancing economic development and gender equity (Devoto et al., 2012; Winter et al., 2021; Wolf et al., 2023). The importance of clean water for human well-being and sustainable development is widely recognized, as evidenced by its inclusion among the United Nations' Sustainable Development Goals (SDG), especially "Goal 6. Ensure availability and sustainable management of water and sanitation for all" (United Nations General Assembly, 2015).

This critical infrastructure has various susceptibilities such as aging, environmental contamination, and potential disruptions due to natural disasters or human activities (Balaei et al., 2020; Birkett et al., 2011; Deng et al., 2020; Sargaonkar et al., 2010). Consequently, there is a significant body of research dedicated to assessing vulnerabilities in these systems in an effort to mitigate risks and enhance the resilience of water supply networks (Haimes et al., 1998; Karamouz et al., 2012; Van Leuven, 2011; Wéber et al., 2020; Zohra et al., 2012).

The resilience of these water supply networks is largely based on the assumption of stable climate conditions. While there may be potential benefits in terms of less frost damage for this infrastructure in colder climates due to global warming (Żywiec et al., 2024), it is essential to recognize a reverse possibility – one of abrupt shifts toward cooler conditions and its implications for water supply network resilience. For example, during a 2021 winter storm in Texas, USA, the sudden drop in temperatures caught many water systems off-guard, leading to frost damage (pipe bursts) and widespread water supply disruptions in areas not accustomed to such cold conditions (Glazer et al., 2021; Grineski et al., 2022; Melaku et al., 2023). One survey found 31% of Texas residents suffered from water damage, and 49% lost access to running water for an average of 52 hours (Watson et al., 2021). Due to low water pressure and water outages potentially compromising drinking water supply, boil water advisories were issued to an estimated 14 million people (Glazer et al., 2021).

Drastic climate cooling can occur from situations such as abrupt sunlight reduction scenarios (ASRSs), e.g. a nuclear winter caused by a nuclear war (Coupe et al., 2019). Nuclear winter is a hypothetical climate phenomenon caused by the injection of large quantities of soot and smoke into the atmosphere, leading to a significant drop in temperature, reduced sunlight, and potentially devastating consequences for global ecosystems and human civilization (Baum, 2015; Turco et al., 1983). Such an event could have a long-term effect on the global climate, with sun-obscuring particulate matter in the upper atmosphere deflecting solar radiation and causing

significant global temperature drops over a 5–10-year period (Coupe et al., 2019; Robock et al., 2007). As we expect a similar decrease in temperature in ASRSs caused by asteroid impacts (Chapman and Morrison, 1994) or large volcanic eruptions (Rougier et al., 2018), the results for our nuclear winter scenario would be applicable to these as well.

Under the conditions set by the most severe variant of such a scenario modeled by Coupe et al. (2019), i.e. the 150 Tg soot one from a nuclear exchange between Russia and the USA, surface light levels remain reduced to less than 40% of normal (i.e. of ~160 W/m^2) for a duration of 3 years, gradually returning to the normal levels over ~10 years. The peak temperature anomaly, occurring around 3 years after the injection, sees global temperatures plummeting to nearly 10°C below baseline levels. Previous studies have analyzed the impact of these conditions on food systems (Denkenberger and Pearce, 2018; Jehn et al., 2024; Xia et al., 2022), but, to our knowledge, this has not yet been done for water supply networks. To thereby expand the understanding of the impact of said extreme conditions, the temperature anomaly was utilized as a baseline for us to analyze potential damage to said networks in such a worst-case scenario.

The potential damage to water pipes from cold temperatures is well documented (Barton et al., 2019; Bruaset and Sægrov, 2018; Rajani and Kleiner, 2001), with a quantifiable correlation between falling temperature and increased failure rates in such infrastructure (Bruaset and Sægrov, 2018; Rezaei et al., 2015; Wols and Thienen, 2016). Rezaei et al. (2015) explains how a decrease in temperature can lead to pipe failures due to volume expansion of water, frost heave in the soil around the pipe, and increased brittleness. Factors such as the intensity and duration of cold weather, as well as water pipe depths influence the development of frost heave. Frost heave and ground freezing typically affect shallowly placed pipe infrastructure more (Farewell et al., 2012; Huang et al., 2022). Thus, we may infer that maximum frost depth increasing as a result of nuclear winter conditions would place a greater amount of underground water supply networks at risk.

To understand the potential damage, it is needed to know the extent of the pipeline. Assessing this extent is challenging. As per Mair et al. (2017), "Urban water infrastructure, i.e. water supply and sewer networks, are underground structures, implying that detailed information on their location and features is not directly accessible, frequently erroneous, or missing. For public use, data is [sic] also not made available due to security concerns. This lack of quality data, especially for research purposes, requires substantial effort when such data is [sic] sought for both statistical and model-based analyses". The challenge is further exacerbated by the fact that infrastructure can vary wildly from country to country, and so does the relevant information (or its lack thereof) in the sources containing the data. Despite the aforementioned recognition of clean water importance, there is no water-supply-network-length indicator in the UN's global indicator framework for SDG[1] adopted so far (United Nations General Assembly, 2017; United Nations

---

[1] Interestingly, we found an instance of a country that presented its street water supply network length as an indicator of achievement of Goal 6 (Federal State Statistics Service, 2019), but such a metric was not reflected in the UN's global framework for the relevant year (United Nations General Assembly, 2017).

Statistical Commission, 2024; United Nations Statistics Division, n.d.). This reliance on country-reported data for measuring the extent of the pipeline could be bypassed by utilising tangential satellite imagery solutions (Asterra, n.d.; Jeffay, 2022; Stantec, n.d.), but such utilisation on a global scale seems unviable.

To overcome these challenges and thus estimate the extent of the water supply networks, we assumed that urban areas are likely to contain such infrastructure and predicted its length based on other variables present in those areas – population size (Pauliuk et al., 2014) and street network length (Mair et al., 2017). The urban areas themselves were determined using datasets on harmonized nighttime lights (Zhao et al., 2022) and global artificial impervious areas (Gong et al., 2020). Given our focus on assessing the capability of the global pipelines to handle the nuclear winter conditions, we predicted the length of this infrastructure overlapping with climate modelling data in the scenario, for the areas with the highest susceptibility to increased freezing. This approach allowed us to identify the scale and distribution of underground water supply networks vulnerable to frost damage, and thus provide a foundational risk assessment of this infrastructure in the nuclear winter scenario.

2. Methods

Given the focus of the study, we had to check whether there are preexisting sources on global pipeline distribution and lengths. As none was found, we created our own datasets.

For the distribution of underground water supply networks, we started with calculating the increase in maximum frost depths expected in the nuclear winter conditions, on a global scale. This allowed us to identify at-risk areas, i.e. those areas in which such an increase would occur. Afterward, we determined which at-risk areas could be also classified as urban ones and thus contain any pipelines. The length of this infrastructure was predicted for each at-risk urban area, and aggregated on a per-country and global basis for results validation and discussion purposes. Our predicted values for the vulnerable countries can be found in the supplementary materials S1 (the current at-risk and historical risk-agnostic lengths) and S2 (the current at-risk lengths, with maximum frost depth breakdowns).

Each following subsection describes the underlying process in detail, except for results validation. Due to the latter's complexity, it is only introduced briefly therein, and expanded on in the supplementary material S3. The flowchart of our methodology is depicted in Fig. 1.

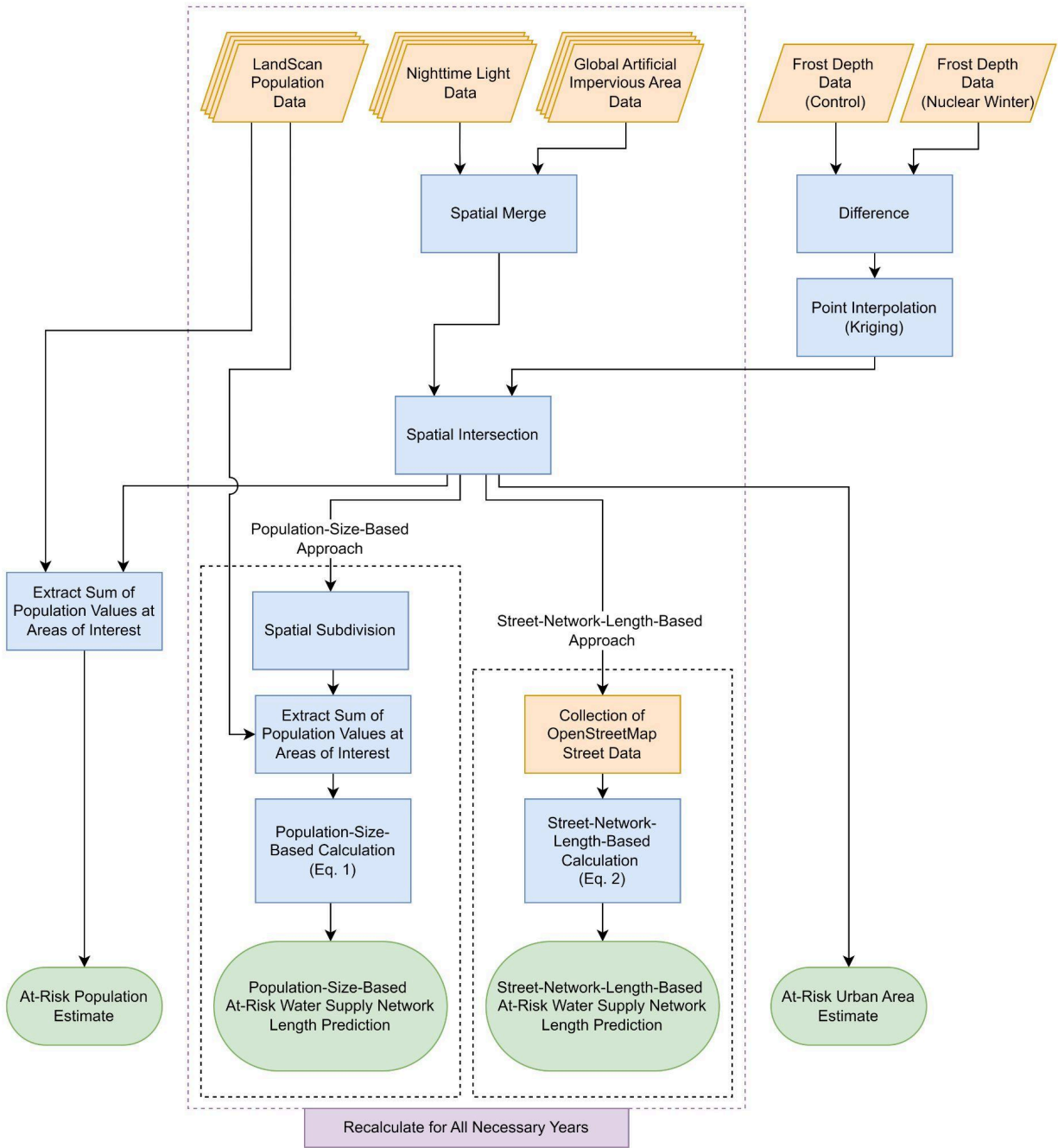Code utilized to create the models of this paper, alongside the various calculations, can be found on the GitHub repository located at https://github.com/allfed/nuclear-winter-water-risk.

Fig. 1. Flowchart presenting an overview of the methodology.

2.1. Water Supply Networks

As we did not find any database or dataset of global underground water supply networks, we attempted to create one using official reported lengths. This attempt was only partially successful due to the lack of complete and unambiguous data for every country we eventually predicted to be at risk in the scenario. Given the difficulties, we settled for obtaining the infrastructure's lengths as described in subsection 2.4. Pipeline Length Prediction, and used the collection for their validation as briefed in subsection 2.5. Pipeline Length Results Validation and elaborated in the supplementary material S3. The collection itself is contained in the supplementary material S1.

Despite the issues, creating the collection informed us about the potential regional or country-specific idiosyncrasies of water supply networks. These were reflected in the variety of rarely-defined terms used by statistical agencies and other governmental bodies, as well as international organizations, water companies, professional associations (including those comprising water companies), and academics, for length indicators within their sources. As we wanted to predict the total lengths of all relevant types of such infrastructure at risk under the nuclear winter conditions – to account for a "worst-case scenario" – we employed an inclusive interpretation of the terms used therein. If a source provided only one relevant term with length datum, e.g. *aqueducts and water distribution networks* (*apeducte și rețele de distribuție a apei*) (Biroul Național de Statistică al Republicii Moldova, 2019), *distribution and transmission mains* (U.S. Environmental Protection Agency, 2018), water pipes (AS Tallinna Vesi, 2019), *water supply pipelines* (National Bureau of Statistics of China, 2019), we treated it as a country-specific synonym of *water supply networks*. In cases of multiple terms with such data not summed in the source, e.g. *house connection pipes* (*Hausanschlussleitungen*) and *supply pipes* (*Versorgungsleitungen*) (VKR - Verband Kunststoff-Rohre und -Rohrleitungsteile et al., 2019), *main water pipe*, *street network*, and *inter-district and inter-yard networks* (Statistical Committee of the Republic of Armenia, n.d.), and *water supply network* and *extension* (Macao Water, 2018), we assumed the terms to describe country-specific constituents comprising such networks.

Moreover, sources authored by the aforementioned entities were mostly agnostic of the water pipe placement, with none breaking down the length in over- vs. underground regard[2], and only two explicitly defining all of such infrastructure as being located in the latter manner (Irish Water, 2015; Republic of Lebanon Ministry of Energy and Water, 2020). Having found no ratios expressing the undergroundness of water supply networks, and other placement types being negligible, for our analysis, we assumed all pipes to be placed fully below the ground surface.

---

[2] It is worth mentioning that there are also other types of placement relevant in the nuclear winter scenario. We encountered official sources mentioning above-ground (Росстат, 2022) and surface (2030 Water Resources Group, 2021) ones, although without data that could be clearly related to the entirety of a given water supply network length.

Despite the assumption that water supply networks are always placed underground, in this study, the term *water supply network* without a placement descriptor means a network in general, i.e. regardless of its placement. Furthermore, *underground water supply network* is used interchangeably with *pipeline*. Unless stated otherwise, we provide all infrastructural terms related to or synonymous with the aforementioned ones as in their corresponding citations. These approaches apply to the manuscript and all supplementary materials.

2.2.   Frost Depth

Using existing climate modelling data from Coupe et al. (2019), we compared the maximum depths at which soil would be expected to freeze, i.e. frost depths (Selezneva et al., 2008), during the nuclear winter scenario, with ones obtained from the control run, simulated to predict maximum frost depths in normal (non-nuclear-winter) conditions.

To validate the results of the control run, the point data were compared with that of National Snow and Ice Data Center (NSIDC) dataset Arctic EASE-Grid Freeze and Thaw Depths (Zhang and Barry, 2006). This dataset had yearly estimated maximum frost depth data with a spatial coverage of the entire Northern Hemisphere (north of 50° N), and a spatial resolution of 25 km. Because this resolution was significantly higher than that of the Coupe et al.'s control data, points were spatially joined by their nearest neighbour. Only points from either dataset that were above land were used. A Pearson correlation coefficient of 0.756 indicated that the data did tend to trend similarly, however, a root mean square error (RMSE) of 1.746 did indicate that the data tended to have a difference of just under 2 m. Ultimately, this was deemed acceptable since a mean error of –0.911 (mean of Coupe et al.'s control data minus NSIDC data) implied that the Coupe et al.'s control data typically underestimated the maximum frost depth, thus underestimating the protective buffer available to the pipes and allowing us to conduct a "worst-case scenario" analysis.

Unless additional measures are implemented (such as heating sources, insulation, special placement solutions, or ones for ensuring continuous flow rates), water pipes are typically located below the local maximum frost depth, or, sometimes, above it to reduce installation costs (Pericault et al., 2017). We assumed the pipelines either did not have such implementations, or if they did, they were only rated for the pipelines' current maximum frost depth – thus, for those placed just below it, even a small increase in maximum frost depth might impact local infrastructure. Therefore, we calculated the difference between existing maximum frost depths in the control run and those predicted for the nuclear winter scenario, allowing us to map potential at-risk areas. In these, infrastructure might not be adequately prepared for the colder conditions.

The nuclear winter climate model data collected came in 1.9° × 2.5° (lat × lon) resolution. To interpolate in-between the data points, we opted for ordinary kriging. This method was chosen due to its ability to effectively estimate data based on neighbouring points, a lack of auxiliary related

variables, and documented success for predicting soil properties (Gia Pham et al., 2019; Ouyang et al., 2013; Pirestani et al., 2024; Zhu and Lin, 2010). All data points over bodies of water were removed so as not to affect the kriging estimate. Of note, the frost depth data provided from Coupe et al. (2019) used the Community Land Model 4.0 as their land surface model, which does take into consideration soil heterogeneity (Oleson et al., 2010). This meant this method was able to consider soil structure when determining frost depths. However, when interpolating in between the data points, the spatial resolution of finer details, such as urban land cover, was lost. Therefore, this process assumed the lack of protection offered by human-made structures, soil structure, and terrain features, when determining the vulnerability of each area to ground freezing.

2.3. At-Risk Urban Area

Urban area estimates are often calculated using a minimum population density approach (Dijkstra et al., 2020), but it may not work for determining urban areas with underground water supply networks. This issue is exemplified by Nigeria, which has a vast urban landscape with the 6th largest population in the world (Oladunmoye, 2024; US Census Bureau, 2024), but only 12% of the total and 15% of the urban population had access to piped water as of 2022 (WHO and UNICEF, 2023). In 2018, 60 million were living there without access to any type of safe water, leading to a state of emergency (World Bank, 2021). Pakistan is in a similar situation: very populous (5th largest) but of low socioeconomic activity (United Nations, 2022; World Bank, 2024a) and low (25% of the total and 39% of the urban population) access to piped water (WHO and UNICEF, 2023). On the other hand, there is the example of the United States of America. Despite a significant variety in population densities between urban, suburban, and rural areas (Pozzi and Small, 2002), piped water access is still readily available to most people even in less populated areas (Meehan et al., 2020). Instead, insecure piped water access is primarily driven by systemic social factors such as precarious housing conditions and poverty (Meehan et al., 2020). Thus, we assumed population-density-based approaches for estimating urban areas with pipelines might overestimate low socioeconomic activity areas while underestimating areas with high-intensity socioeconomic activity but lower population density. Consequently, we sought a different approach.

Instead of using a population-density-based approach, we merged urban area extents derived from harmonized nighttime lights (NTL) and global artificial impervious areas (GAIA), developed and provided by Zhao et al. (2022) and Xuecao et al. (2020), respectively. While the former dataset was based on data collected by the U.S. Air Force Defense Meteorological Satellite Program Operational Linescan System (Zhao et al., 2022), the latter used imagery from Landsat 8 and the Sentinel-1's synthetic-aperture radar (Gong et al., 2020; Xuecao et al., 2020). The NTL-based urban area was described as best defining the "spatial extents associated with intensive human settlement and high-intensity socioeconomic activities" (Zhao et al., 2022). This meant that the NTL data were less likely to capture areas with a high population density but low socioeconomic activity (such as

Nigeria and Pakistan), while being more likely to capture lower density suburban areas across North America and Europe, and thus might more likely correlate with areas containing pipelines.

The idea of using NTL data for predicting areas with underground water supply networks was supported by Zhao et al. (2011), which found strong positive correlations between observed lit area and total water footprint, domestic water withdrawal, and industrial water consumption.

Although the NTL dataset encompassed the majority of the area of interest, manual inspection revealed its deficiency in covering lower-lighting intensity cities in Europe and North America. Initially, the GAIA-based urban area estimate was poised to supplant the NTL data due to their similar coverage, with GAIA capturing the lower-intensity cities. Artificial impervious areas can be defined as human-made structures, such as pavements, roads, buildings, and other infrastructure, that impede the natural flow of water into the soil (Gong et al., 2020). These attributes likely allowed the dataset to capture the lower-intensity but more affluent areas that the NTL dataset was probably missing. However, upon closer examination, the GAIA dataset tended to overlook rural, higher intensity, and wealthier residential suburban or acreage districts in Europe and North America. Despite typically having underground water supply networks, these residential areas often had expansive yards that were not artificially impervious. Both datasets effectively avoided overcapturing high-populated but low-socioeconomic activity areas, where such water infrastructure is not typically found. Consequently, the datasets were spatially merged (only one dataset needed to cover the space to consider it likely to contain a pipeline). The combined ability of the NTL and GAIA datasets to cover urban areas likely to have underground water supply networks, while excluding urban areas unlikely to do so, is exemplified in Fig. 2, Fig. 3, and Fig. 4.
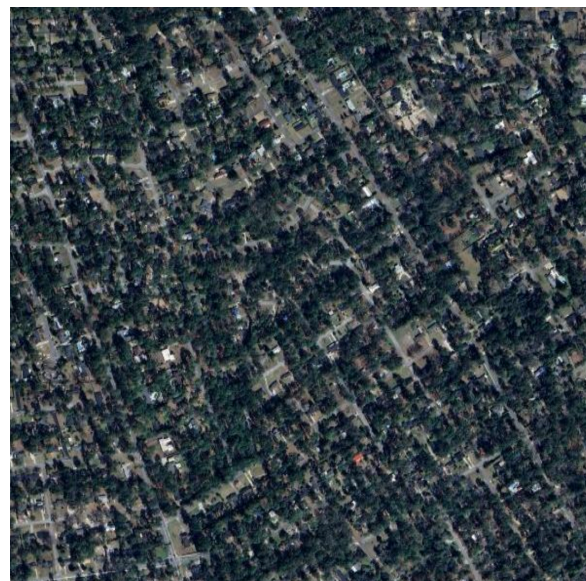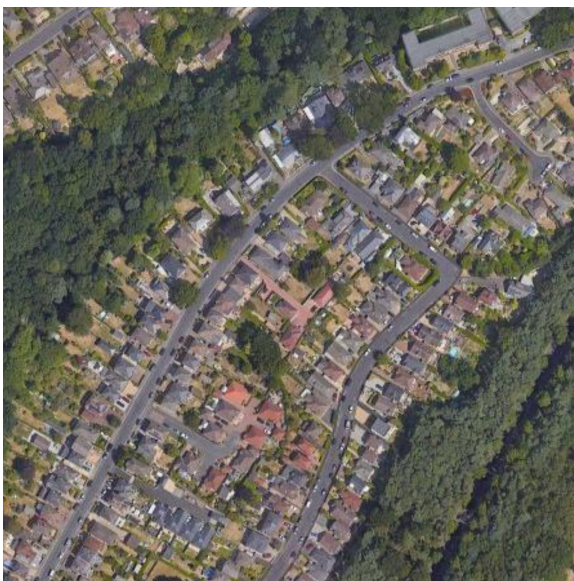
Fig. 2. Neighbourhood in Bournemouth, UK (Google, 2024a). Not captured by the NTL dataset, but captured by the GAIA dataset. Imagery ©2024 Airbus, Maxar Technologies, Map data ©2024.

Fig. 3. Neighbourhood in Valdosta, Georgia, USA (Google, 2024b). Not captured by the GAIA dataset, but captured by the NTL dataset. Imagery ©2024 Airbus, Maxar Technologies, Map data ©2024.

Fig. 4. Town of Nasirabad, Pakistan (Google, 2024c). Not captured by either GAIA or NTL datasets. Imagery ©2024 Airbus, CNES / Airbus, Maxar Technologies, Map data ©2024.

In order to validate our assumptions that these datasets were able to accurately estimate areas with said networks, we calculated the population of these urban areas per country using 2023 LandScan (latest available) population raster imagery (Lebakula et al., 2024), a widely used global population raster choice with demonstrated success in disaster scenarios (Jordan et al., 2010; Rose and Bright, 2014). These were compared with the WHO/UNICEF Joint Monitoring Programme for Water Supply, Sanitation and Hygiene (JMP)'s estimates of the proportion of country population using improved piped water supplies, for both rural and urban areas (WHO and UNICEF, 2023)[3]. Our per-country prediction of populations with piped water achieved an R^2 value of ~0.80 when

[3] The population data used in JMP was based on the work of the United Nations Population Division (WHO and UNICEF, 2021). The most probable source (United Nations, Department of Economic and Social Affairs, Population Division, 2019) of such data presented a complex landscape of what was used by countries to differentiate urban areas from rural ones. Among the provided criteria were, sometimes solely, administrative designations, population size or density, economic characteristics, and functional characteristics. The last criterion was used in less than a third of cases, of which an unspecified number related the definition to the existence of water-supply systems therein. This uncertainty in what constituted urban areas further supported our need of employing a different method for identifying them.

compared with the corresponding JMP estimate. The remaining variability could stem from numerous factors, including variations in the JMP survey estimates, households with access to piped water located not on their premises, inexact predictions from the NTL and GAIA datasets, and differences in underground infrastructure patterns across a wide range of urbanized areas globally. In order to verify that this approach was able to recognize changes in global piped water access, which has risen significantly over the past ~30 years (Milman et al., 2021), we compared our estimate with those of JMP, for the years 2000, 2005, 2010, 2015, and 2018 (years when all the data were available), and the R^2 score remained between 0.73 and 0.80.

In the next step, we looked for the intersection between the areas that were likely to have underground water supply networks (i.e. urban areas) and the previously calculated at-risk areas.

2.4. Pipeline Length Prediction

Having determined the global area that would likely contain underground water supply networks and be impacted by the increase in maximum frost depth in the nuclear winter scenario, the amount of such infrastructure within the area could finally be predicted. In order to do so, we used two different approaches (one based on population size and one on street network length) and compared the results.

2.4.1. Population-Size-Based Approach

An approach of estimating water supply network length was proposed by Pauliuk et al. (2014). The authors developed a hierarchical fractal model for water pipeline networks and calibrated it using empirical data from 35 cities in 5 countries throughout 3 continents (with served populations ranging from 500 to ~23,000,000 inhabitants). Via their model, a relationship between population of a city and length of its water supply network was found; for our analysis, we expressed it as in Eq. (1):

$$L_{pipe,i}^{(population-size-based)} = 0.01\ Pop_i^{0.9} \tag{1}$$

where $L_{pipe,i}^{(population-size-based)}$ and Pop_i are the water supply network length predicted with the population-sized-based approach [km], and total population, respectively, of a region i.

In order to apply it to our global data, the multipolygon geographic bounds of our at-risk urban areas were exploded, such that each polygon could represent an individual urban area. The original study considered actual city areas, while ours employed rough urban boundaries. To achieve a

closer approximation of city boundaries for each polygon, each polygon was subdivided to ensure that no area exceeded the municipality area of São Paulo – i.e. 1,521 km^2 (Instituto Brasileiro de Geografia e Estatística, n.d.) – the largest city in the original study. Although global rankings of largest cities could vary significantly due to differing administrative units in different parts of the world, São Paulo was regularly ranked amongst one of the largest (Forstall et al., 2009; Moriconi-Ebrard, 1991; Taubenböck et al., 2019). Thus, by subdividing areas larger than that of São Paulo's administrative area, we could break apart urban areas that were likely to be made up of various municipalities since individually they were unlikely to surpass São Paulo's area. For each of these polygons, the respective population was calculated using the 2023 (latest) LandScan raster (Lebakula et al., 2024). Eq. (1) was then applied individually to each polygon and then summed up to arrive with this approach at per-country and global pipeline lengths at risk.

2.4.2.   Street-Network-Length-Based Approach

A correlation between lengths of street network and water supply network was found in Mair et al. (2017). The authors arrived at an estimate of 50% of the former coming with 78% of the latter[4], i.e. 1 km of street network coming with ~0.641 km (i.e. 0.5/0.78) of water supply network.

Mair et al.'s technique for determining street network length through the use of OpenStreetMap was replicated on a global basis for the previously determined at-risk urban area. This included using the same definition of street network, wherein all available streets found in OpenStreetMap were used. In OpenStreetMap terms, this meant collecting all "ways" with a key of "highway", which encompassed any kind of street, road, or path, including but not limited to major highways and motorways, residential streets, rural roads, and pedestrian paths (OpenStreetMap contributors, 2024). Notably, this caused additional paths – such as sidewalks and parking lots – that may not typically be considered "streets" to potentially be included in the street length calculations, thus accounting for the pipes underneath more types of infrastructure.

After determining the street network length for each at-risk urban area, we employed Mair et al.'s estimate as in Eq. (2) to predict the pipeline length within:

---

[4] In its Figure 5, Mair et al. (2017) indicated the average values of "streets containing water supply pipes" of 50%, and "water supply pipes below the street" of 78%. While discussing the results, the authors stated that "approximately 50% of the street network contains 78% of the water supply or sewer network", even though the Figure depicted 48% for "streets containing sewer pipes" and 85% for "sewer pipes below the street"; in other places of the paper, it was concluded that "50% of the street network length correlates with 80%–85% of the total water supply/sewer network". To address this discrepancy, we decided to use the most specific values, i.e. 50% for street network and 78% for water supply network, especially since Mair et al. seemed to treat "water supply pipes" as synonymous with the latter.

$$L_{pipe,i}^{(street-network-length-based)} = (0.5/0.78)\ L_{street,i} \qquad (2)$$

where $L_{pipe,i}^{(street-network-length-based)}$ and $L_{street,i}$ are the water supply network length predicted with the street-network-length-based approach [km], and street network length [km], respectively, of a region i.

Notably, our method was designed to determine the spatial variability of at-risk pipelines, not just between whole countries, but within them as well. Frost depth in the nuclear winter scenario alongside infrastructure density could change drastically from one area in a country to another, which is why we did not simply multiply country-wide street network lengths by the ~0.641 estimate.

To arrive with this approach at per-country and global underground water supply network lengths at risk, we summed up the results of Eq. (2) applied individually to each at-risk urban area.

2.5. Pipeline Length Results Validation

To validate the capabilities and compare the results from both prediction approaches, we used the aforementioned collection of country-wide reported water supply network lengths, which can be found in the supplementary material S1. In this subsection, we briefly introduce the validation process – its methods, results, as well as limitations and uncertainties are described extensively in the supplementary material S3.

Having in mind the largely different scales between countries' infrastructure, we compared the logged values of the predicted lengths against the logged values of the corresponding reported ones, and obtained the R^2 of logged values from the population-size-based and the street-network-length-based approaches (separately). In both cases, the predictions were made for the country's urban areas (i.e. not limited to its at-risk ones), and only for the year as of which the length was reported. Due to the limited availability of reported data and matching yearly versions of the datasets required for predicting, no such prediction was made for a year later than 2018. To better understand how close each predicted length was to the relevant reported one, we also calculated the logged values of the predictions against the logged values of the reported lengths, essentially calculating the root mean squared logged error (*RMSLE*).

As completing the collection for all countries that were recognized to be at risk in the scenario turned out not to be viable, we had to check whether the limited sample was likely to be representative of the remaining countries. For this, we utilized bootstrapping to assess the consistency of the R^2 and *RMSLE* values for the relationship between predicted and reported lengths.

In case of a poor predicting performance of an approach in one or many of the validation tests, we decided to scope the discussion on the length results obtained via the other one.

2.6. Vulnerability of Selected Countries

Although our main focus was on the global extent of the pipeline at risk in the scenario, we also looked into the 20 countries with the highest predicted lengths of this infrastructure and compared them with the summed value for the rest of the world. Moreover, to better understand the potential impact of the nuclear winter conditions, we computed the at-risk underground water supply network lengths per capita and per GDP (separately). Population and GDP values for each country were sourced from the World Development Indicators (World Bank, 2024b, 2024c).

3. Results and Discussion

3.1. At-Risk Areas and At-Risk Urban Areas

In Fig. 5, the at-risk areas are presented on a global scale. Notably, only countries in the Northern Hemisphere would experience an increase in maximum frost depth under the nuclear winter conditions. Far-northern areas, mostly within the Arctic Circle – such as in Greenland, Canada, and Russia – would not see an increase in maximum frost depth, as they often already experience deep permafrost (Romanovsky et al., 2002).
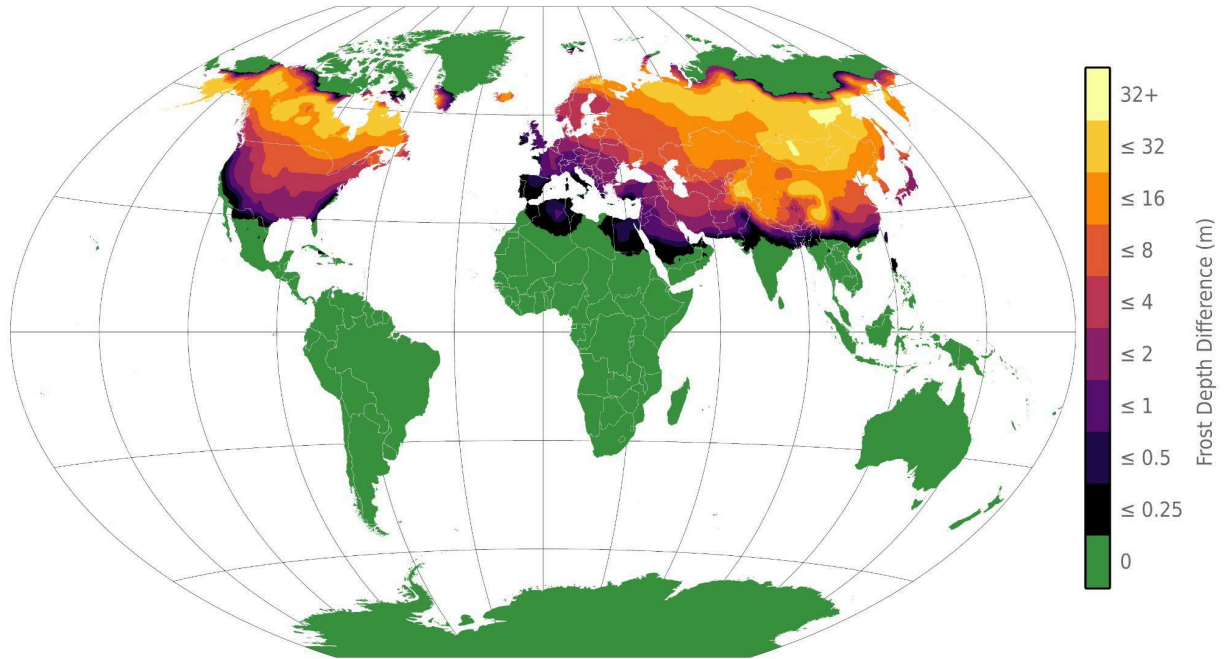
Fig. 5. Map of difference between control maximum frost depth and maximum frost depth in the nuclear winter scenario. At-risk areas have a positive difference.

The at-risk areas that are also determined to be urban ones are depicted in Fig. 6. The total calculated at-risk urban area is ~1,289,499 km². The majority of urban areas north of the 25th parallel north would be impacted, with regional variations throughout. As there are few urban settlements in the Arctic Circle, most of the impact occurs between the 25th and 65th parallel north.
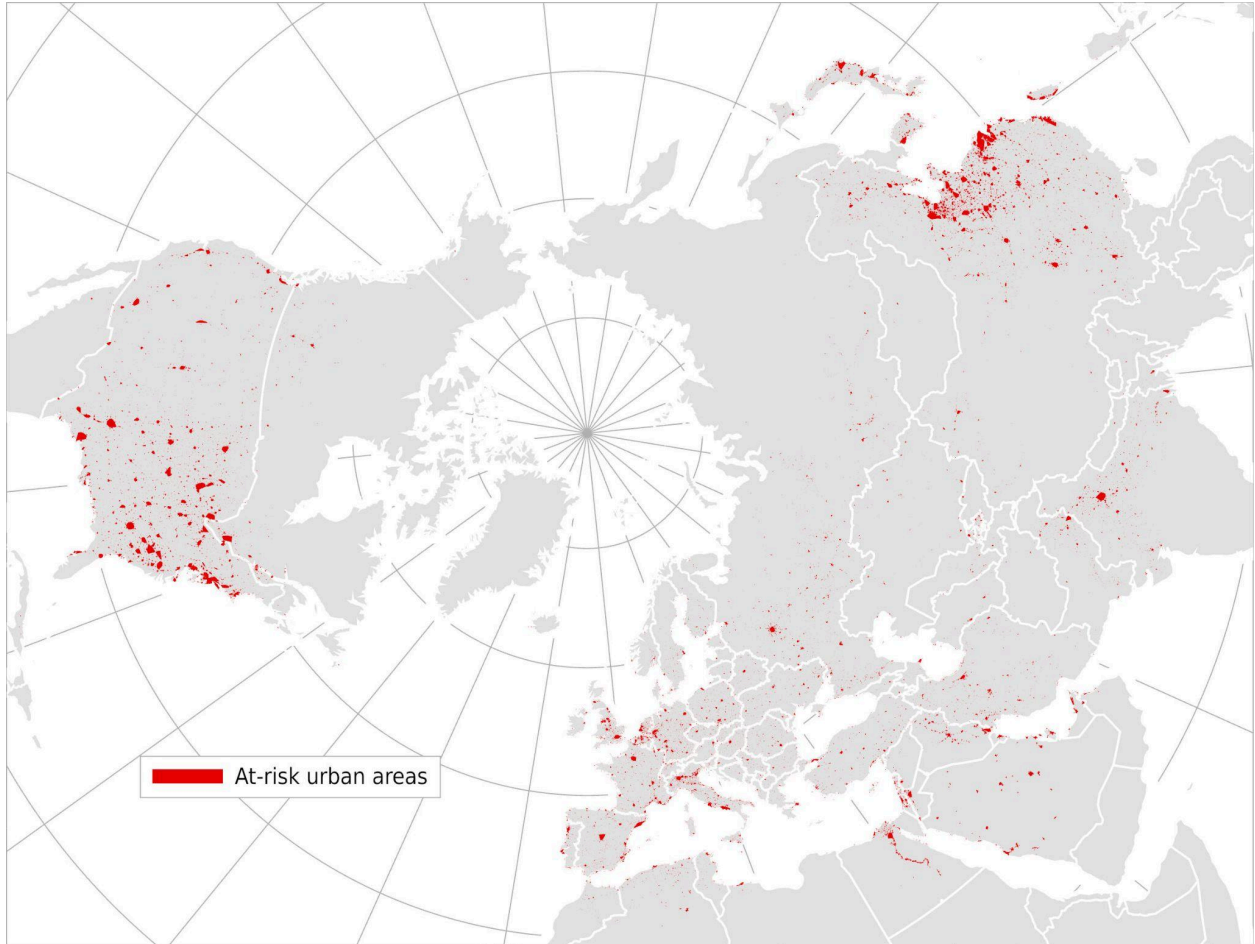
Fig. 6. Map of at-risk urban areas (areas with underground water supply networks, at risk in the nuclear winter scenario).

3.2. Pipeline Length Predictors

Within the at-risk urban areas, there would be a total of ~2.1 billion people who may lose access to their primary water source. It is crucial to acknowledge that there may be cascading effects as networks lose connections, potentially affecting individuals living just outside these areas and leading to additional loss of water access. In addition, deeper ground freezing could affect people with wells that are not directly underneath heated buildings. Moreover, individuals who collect water directly from surface water features would be affected by increased freezing. Thus, we assume the estimate of ~2.1 billion at-risk individuals for the specific nuclear winter scenario to be conservative.

In the at-risk urban areas, the total street network length is determined to be of ~13.7 million km, entailing a network density of ~10.7 km of street for every square kilometer of land. This seems to be a reasonable value, since the OECD's estimates for road density have it sitting at ~0.1–4 km of road for every square kilometer of land for each country (in its sample of 50 countries), including both urban and rural land (OECD, 2024) while our result is only for urban areas (likely to have a denser street network).

3.3.   Global Pipeline Length

The global results of both at-risk underground water supply network length prediction approaches are presented in Table 1. The supplementary material S2 provides the predicted length per country, and per maximum frost depth difference per country. Whether a country would be fully composed of at-risk areas, and thus all of its pipelines be affected, is specified in the supplementary material S1 which, for ease of reference, also contains the at-risk lengths per country.

Approach	Global Underground Water Supply Network Length at Risk [km]
Population-size-based (Pauliuk et al., 2014)	~5,355,411
Street-network-length-based (Mair et al., 2017)	~8,810,888

Table 1. Predicted length of the global underground water supply network at risk in the nuclear winter scenario, per approach used.

Despite using two different techniques with differing data sources for determining the global pipeline length, the two predictions remained within the same order of magnitude, achieving a percentage difference between them of ~49%. This consistency raises our confidence that the results are reasonably close to reflecting the reality of the infrastructure length at risk in our hypothetical nuclear winter.

As can be seen in the supplementary material S3, across Table S3.1, Fig. S3.2, and Fig. S3.3, overall, the street-network-length-based predictions perform better in both statistical tests (higher R^2 and lower *RMSLE*) while simultaneously maintaining more stable results in the bootstrapping analysis, when compared with the population-sized-based one. Thus, the length results predicted with the former approach are discussed henceforth.

Using the better predictor – street network length – we arrive at an average total of ~6.76 km of underground water supply network per square kilometer of land in our calculated at-risk urban area.

3.4.   Most Vulnerable Countries

A closer look at how selected countries would be affected in terms of its at-risk pipeline length can be taken via Fig. 7; in terms of its at-risk pipeline length per capita, via Fig. 8; in terms of its at-risk pipeline length per GDP, via Fig. 9. The Figures also present a frost-depth-difference breakdown of each length.
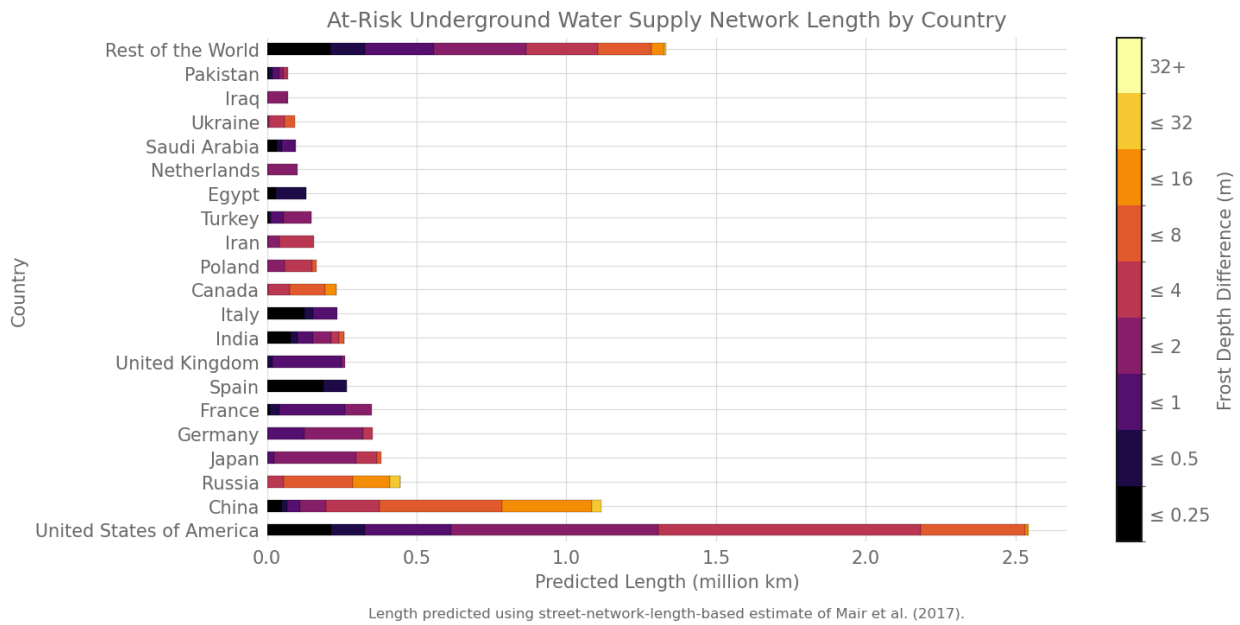

Fig. 7. Underground water supply network length by country, at risk in the nuclear winter scenario. The 20 countries with the highest values and the summed value for the rest of the world are depicted.

At-Risk Underground Water Supply Network Length by Country per Capita

Length predicted using street-network-length-based estimate of Mair et al. (2017).
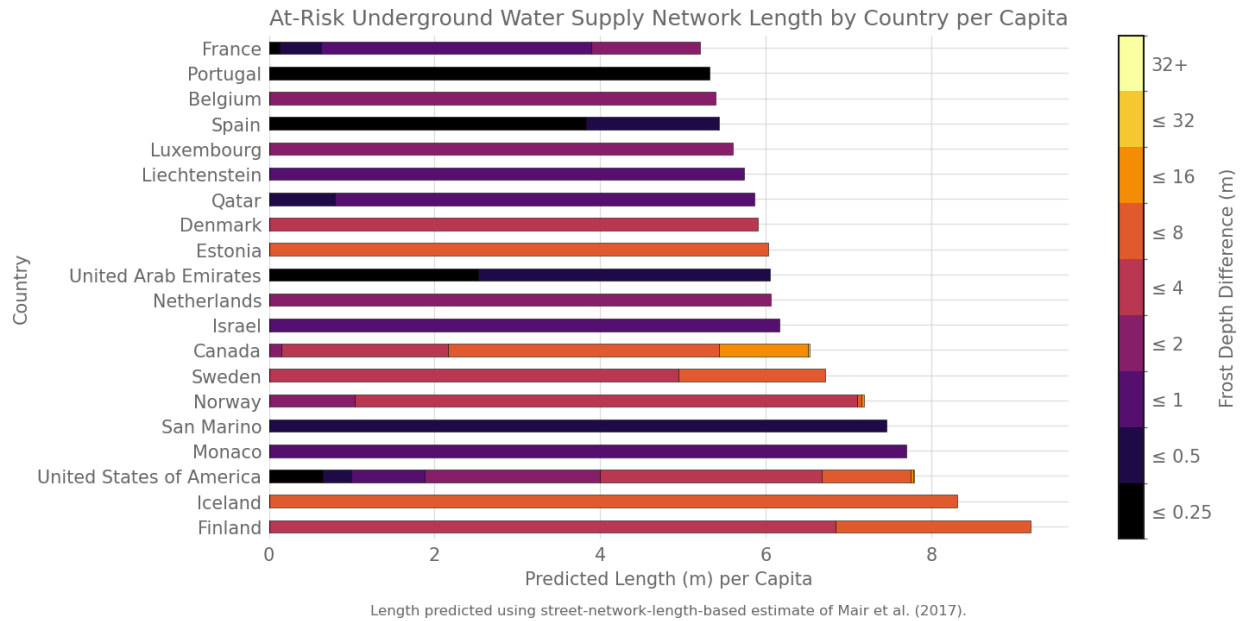
Fig. 8. Underground water supply network length by country per capita, at risk in the nuclear winter scenario. Only the 20 countries with the highest values are depicted.
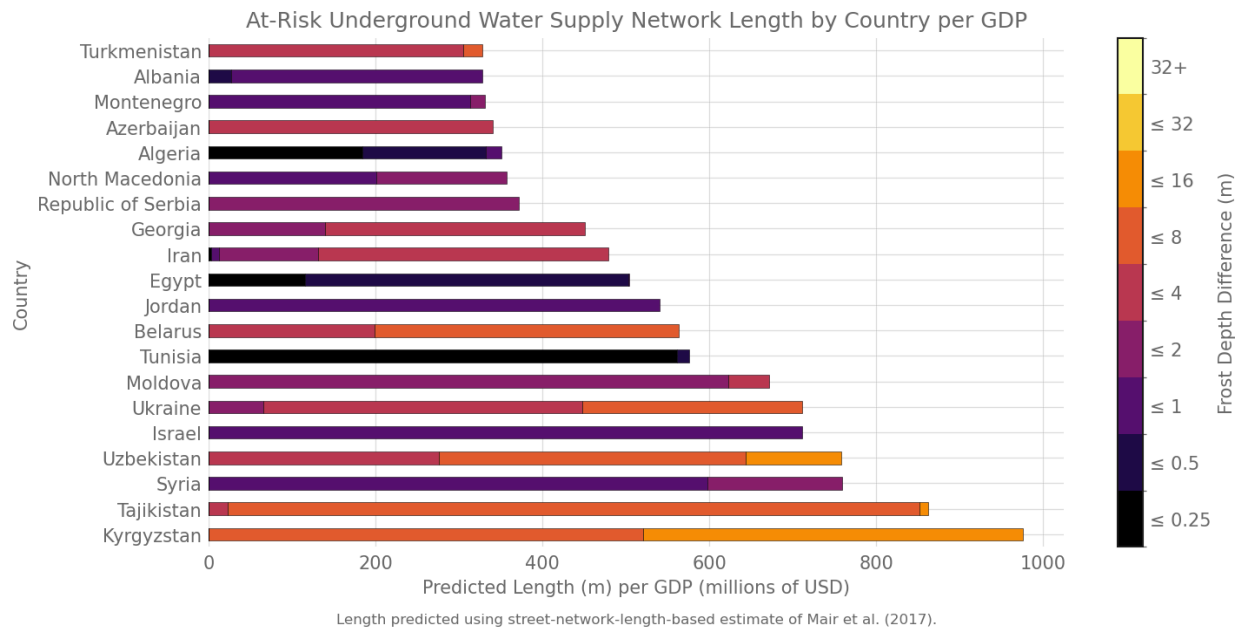

At-Risk Underground Water Supply Network Length by Country per GDP

Length predicted using street-network-length-based estimate of Mair et al. (2017).

Fig. 9. Underground water supply network length by country per GDP, at risk in the nuclear winter scenario. Only the 20 countries with the highest values are depicted.

From the per-GDP calculation, we may be able to better understand how capable each country would be at handling the significant challenge occurring in the scenario. From the top 20 countries with respect to their at-risk pipeline length per GDP, Kyrgyzstan, Tajikistan, Syria, Uzbekistan, Tunisia, Jordan, and Egypt are classified as lower-middle income or low income ones (World Bank, 2024a), potentially making them particularly vulnerable to the nuclear winter conditions.

Canada, China, Russia, the USA, and Mongolia are the only countries with underground water supply networks where the maximum frost depth would increase by more than 20 m. India, Kazakhstan, Kyrgyzstan, North Korea, Uzbekistan, and Norway join them as countries with pipelines where such an increase would occur by more than 10 m. Of the 92 at-risk countries, 34 would have their frost depth increased by 1 m or less.

Through our analysis, we demonstrate that a significant portion of the Northern Hemisphere's underground water supply network would be vulnerable to frost damage under the nuclear winter conditions. There are certain countries that stand out:

- The USA holds the highest at-risk pipeline length at ~2,544,308 km. This is more than double the second place, China, at ~1,116,619 km.

- Most of the top 20 countries with a high proportion of at-risk underground water supply networks compared with their population are European, including all Nordic sovereign states (Finland, Iceland, Norway, Sweden, and Denmark). From outside of Europe, they are joined by the USA, Canada, Israel, the United Arab Emirates, and Qatar. (Listings in order of at-risk pipeline length by country per capita).

- Several countries may be particularly vulnerable due to low GDP. This includes various post-Soviet sovereign states such as Kyrgyzstan, Tajikistan, Uzbekistan, Ukraine, Moldova, Belarus, and Georgia, alongside various Middle Eastern countries such as Syria, Israel, Jordan, and Iran. (Listings in order of at-risk pipeline length by country per GDP, after the grouping).

3.5.   (Cross-)System Susceptibilities

It is important to recognize indirect water supply network vulnerabilities as well as potential cascading effects from frost damage on the pipelines. We can draw parallels between the climate-change-focused research of van Thienen et al. (2023) and the potential implications of the nuclear winter to get a better understanding of such vulnerabilities in the hypothetical conditions. That analysis emphasizes the importance of understanding water supply systems' role for continuously providing the essential service in societal collapse scenarios, and – by utilizing a risk matrix approach from NASA (2017) – categorizes the risk to water sector entities as ranging from moderate to extreme. It also identifies several vulnerabilities specific to water supply and

infrastructure in a societal collapse scenario by comparing it with those in fragile and conflict-affected states, as outlined by Bolton (2020). The scenario includes, among others, increased water demand due to displaced populations, loss of skilled personnel, physical infrastructure damage, reduced electricity availability, and financial sustainability challenges for water companies. While our paper primarily focuses on physical infrastructure damage, specifically to water pipes due to frost, each of the other possible vulnerabilities identified would also be prevalent in a nuclear winter scenario. This holds true even beyond the regions with a predicted increase in maximum frost depth, and thus countries not specifically highlighted in this study may still need, in the face of such scenarios, to assess resilience of their water supply networks and associated infrastructure.

Additionally, Kadri et al. (2014) underscores the role of water pipes as physical links in the interdependency of critical infrastructure systems, as highlighted in their framework Cascade Effect Analysis. To illustrate, the 2021 winter storm in Texas exemplified the cascading effects of extreme weather events on infrastructure. As much of the region's energy system was dependent on water remaining in a liquid state (Glazer et al., 2021), drastic temperature drops caused power outages, which, in turn, impacted public water systems. Moreover, frozen water pumps forced a nuclear power plant to shut down, exacerbating the power outages and further disrupting the water supply and treatment systems (Melaku et al., 2023). These sorts of interconnected impacts are likely to occur globally in the event of a nuclear winter, but may have a greater prevalence in our identified at-risk areas.

Lastly, it is worth pointing out that water supply disruptions may not render the resource contained within the pipeline completely unobtainable. For crisis situations, Szpak and Szczepanek (2023) proposes water supply companies to preemptively install drain wells at the lowest points of the water supply system. If water pressure in the network would be too low for the resource to reach the end users, water would flow from a pipe into the nearest drain well, and eventually be transported to the surface using a portable submersible pump. Although we recognize that this should be done only shortly after the onset of a crisis situation or in prospect of one, low and negative pressures occurring within the pipelines can be associated with increased contamination risk (LeChevallier et al., 2003). If ensured to be free of health-related hazards, the water obtained via the drain well method from a single pipe with a length of 1 km and a diameter of 0.3 m has a potential to meet the daily physiological need for water of 2.5 l per capita per day (Szpak and Szczepanek, 2023) of ~28,000 people.

3.6. Limitations and Uncertainties

Our analysis is subject to several limitations warranting consideration, as it does not consider:

- Variability in infrastructure characteristics: Our study is agnostic in terms of the differences in pipe features such as diameter, insulation, and material composition. These factors may play a role in determining the resilience of underground water supply networks to changing climate conditions and could impact the extent of damage experienced under the nuclear winter scenario.

- Relation between other pipeline–ground-surface orientation and freezing vulnerability. We assumed that pipes are parallel to the ground surface, and located just below current maximum frost depths. In reality, parts of the infrastructure would cross through frost depths and thus be at risk in a non-uniform way, e.g. the closer to the surface the more vulnerable to freezing a pipe section would be (in general).

- Freezing vulnerability of ground. Due to the interpolation employed in identifying at-risk areas, ground (and thus the pipelines therein) was considered to be uniformly vulnerable to freezing. Therefore, any protection offered by human-made structures, soil structure, or terrain features is not reflected in the predicted lengths, although it is likely to be a factor in the scenario.

- Duration of ground freezing: Our analysis does not account for the duration of ground freezing under the nuclear winter conditions. The study was based on the assumption that pipes located in areas where the maximum frost depth would not increase would be safe from frost damage.

- Scenario-specific changes in pipeline length: We assumed the extent of the infrastructure to be unaffected by the cause and development of the ASRS and thus see the results applicable to any such scenario with a similar decrease in temperature. However, many Northern-Hemisphere urban areas would probably be destroyed with nuclear or other weapons in the 150 Tg nuclear war (Toon et al., 2008) before even being susceptible to frost damage. Depending on the area of impact, the other potential sources of ASRS – asteroid collisions and large volcanic eruptions – may have significantly lower direct effect on the underground water supply network length. Similarly, we assumed no additional construction or reconstruction of the pipelines.

Moreover, we acknowledge the following uncertainties of our analysis:

- To address the unavailability of underground water supply network distribution and length data, the study relies on a combination of nighttime lights and artificial impervious areas as a proxy for urban areas, which in turn proxy for areas containing such networks. This introduced inherent variability in our results and could affect the accuracy of the vulnerability assessments.

- Despite its better predicting performance in our validation tests, Mair et al. (2017)'s model correlating street network length with pipeline length relies on data pertaining to "three

case studies in an alpine region with different network sizes" which might not be representative of the infrastructure in the whole at-risk area. Moreover, we had to choose between discrepant correlation values presented in that study. If the choice does not reflect those intended by its authors, our predictions would be slightly affected.

- Due to lack of yearly versioning of some datasets, those used for predicting current underground water supply network lengths were never as of the same year. In order to mitigate the issue, we utilized the latest datasets and assumed that no significant change occurred in between the corresponding as-of years.

- The extent of the consumer endpoints of pipelines in the predicted lengths is highly unknown. Even though Mair et al. (2017)'s and Pauliuk et al. (2014)'s models accounted for household or private connections, respectively, the studies did not address whether such connections were the final underground pipes before the end user. If we take the information from DANVA (2019) and Water UK (2022) as representative of the whole at-risk urban area, water suppliers – due to external ownership and leakage responsibility – often have limited knowledge on the condition and length of the property owners' parts of consumer endpoints. Therefore, the predicted lengths at risk in the scenario should be treated as conservative.

4. Future Work

We collected reported pipeline lengths merely to validate the results that used Pauliuk et al. (2014)'s and Mair et al. (2017)'s models. A future work could compare such reported data with reported population sizes and reported street network lengths, for urban areas, and thus correlate the variables more accurately. For the underground context, this could be improved even further if reported water supply network length values were broken down by placement types. Such a breakdown in itself would greatly inform infrastructure protection endeavours. For the time being, the street network length seems to be the better predictor in urban areas.

Although we deemed pipelines vulnerable if any increase in maximum frost depth would occur at their location, a more comprehensive vulnerability assessment would investigate the relation between pipe diameter and frost depths resulting in partial or total freezing of the former, and consider the extent of freezing affecting the infrastructure and its operations. Such assessment could factor in the water supply network idiosyncrasies across regions and countries. It may be beneficial to focus on such scales and also look into the pipeline occurrence beyond the urban areas proxied herein. Targeted analyses may be able to better capture features influencing the infrastructure's vulnerability in such ASRSs. Our paper provided a foundation for identifying at-risk areas – and countries – which may benefit from these context-specific assessments.

Furthermore, future works should look into potential damage to water supply networks beyond frost impacts. While our study was primarily focused on the vulnerability of pipelines to frost damage under the nuclear winter scenario, it is essential to recognize that infrastructure may still be susceptible to damage even if not directly frozen, e.g. to power outages, as discussed in subsection 3.5. Additional Considerations.

A future study should also look into the resilience of other piped systems related to the water availability and quality, e.g. sewer networks involved in wastewater treatment. This process is to reduce contaminant levels below sectoral quality thresholds for intentional reuse, and may augment water supply for human use (Jones et al., 2021). As, on a global basis, ~52% of produced and ~84% of collected wastewater is estimated to be treated (Jones et al., 2021), preserving the continuity of these processes could significantly increase the water available in specific catastrophic scenarios. Predicting the underground sewer network length can be done via dedicated models (Mair et al., 2017; Pauliuk et al., 2014), plausibly with limitations similar to the aforementioned water-supply-network ones. In the context of the nuclear winter conditions, we expect sewer networks to greatly differ in susceptibility to maximum frost depth increase, due to the seemingly higher pipe placement variability (Bi et al., 2022; Brush et al., 1924; Mayny et al., 2024; Pericault et al., 2017).

Lastly, addressing the vulnerabilities described in this paper necessitates exploring potential options to maintain the integrity and functionality of underground water supply networks. Under the nuclear winter conditions, many freeze protection measures described by Pericault et al. (2017) may be leveraged, e.g. heating the water before it enters the network, incorporating electric resistance heating (heat taping), insulating the pipelines (through traditional insulation methods surrounding the pipes or, as we suggest, by covering them with materials such as soil, biomass, or gravel), or by relocating the pipes further underground. Likely, a variety of context-specific methods would need to be adopted to address the diverse challenges at each pipe's location. The viability assessment of protective measures is planned for a later study.

5. Conclusion

Our study sheds light on a critical aspect often overlooked in current water risk research: the vulnerability of the global underground water supply network to sudden catastrophic climate changes, specifically those related to significant decreases in temperature, as in abrupt sunlight reduction scenarios. The analysis reveals a concerning picture, indicating that ~5–9 million km of such crucial infrastructure across 92 countries would be vulnerable to frost damage under such a scenario, potentially leaving over 2 billion individuals without access to clean water. The results serve as a starting point for future works on determining the effect on pipelines in abrupt shifts toward cooler conditions, especially taking into account infrastructure idiosyncrasies of at-risk areas.

Acknowledgements

References

2030 Water Resources Group, 2021. Mongolia: South Gobi region: Hydro-economic analysis: Prioritized solutions for demand reduction and supply augmentation in the mining and heavy industry region in South Gobi [WWW Document]. URL http://documents1.worldbank.org/curated/en/099092723115040780/pdf/P17148804f8d7505 909208015fd451e8a46.pdf (accessed 9.1.24).

AS Tallinna Vesi, 2019. Consolidated annual and sustainability report for the financial year ended 31 December 2018 [WWW Document]. URL https://tallinnavesi.ee/wp-content/uploads/2019/03/TV_Annual_Report_2018_ENG_final.pd f (accessed 8.30.24).

Asterra, n.d. MasterPlan: Pipe Deficiency Assessment [WWW Document]. Asterra. URL https://asterra.io/solutions/masterplan/ (accessed 12.15.24).

Balaei, B., Wilkinson, S., Potangaroa, R., McFarlane, P., 2020. Investigating the technical dimension of water supply resilience to disasters. Sustain. Cities Soc. 56, 102077. https://doi.org/10.1016/j.scs.2020.102077

Barton, N.A., Farewell, T.S., Hallett, S.H., Acland, T.F., 2019. Improving pipe failure predictions: Factors affecting pipe failure in drinking water networks. Water Res. 164, 114926. https://doi.org/10.1016/j.watres.2019.114926

Baum, S.D., 2015. Winter-safe deterrence: The risk of nuclear winter and its challenge to deterrence. Contemp. Secur. Policy 36, 123–148. https://doi.org/10.1080/13523260.2015.1012346

Bi, W., Wang, W., Wang, R., Cui, Z., 2022. Comparison and selection of sewage deep tunnel engineering schemes based on value engineering. Value Funct. Cost 2. https://doi.org/10.54517/vfc.v2i2.2582

Birkett, D., Truscott, J., Mala-Jetmarova, H., Barton, A., 2011. Vulnerability of water and wastewater infrastructure and its protection from acts of terrorism: A business perspective, in: Clark, R.M., Hakim, S., Ostfeld, A. (Eds.), . Springer New York, New York, NY, pp. 457–483. https://doi.org/10.1007/978-1-4614-0189-6_23

Biroul Național de Statistică al Republicii Moldova, 2019. Activitatea sistemelor centralizate de alimentare cu apă şi de canalizare în anul 2018 [WWW Document]. URL https://statistica.gov.md/ro/activitatea-sistemelor-centralizate-de-alimentare-cu-apa-si-de-canalizare-9780_3164.html (accessed 7.26.24).

Bolton, L., 2020. Water infrastructure in fragile- and conflict-affected states [WWW Document]. URL https://www.washcluster.net/sites/gwc.com/files/2022-01/Water_infrastructure_in_fragile _and_conflict-affected_states.pdf (accessed 1.31.24).

Bruaset, S., Sægrov, S., 2018. An analysis of the potential impact of climate change on the structural reliability of drinking water pipes in cold climate regions. Water 10, 411. https://doi.org/10.3390/w10040411

Brush, W.W., Brockway, W.C., Ruggles, A.V., 1924. Laying water mains or services in trenches with sewer pipe. J. AWWA 11, 255–256. https://doi.org/10.1002/j.1551-8833.1924.tb14247.x

Chapman, C.R., Morrison, D., 1994. Impacts on the Earth by asteroids and comets: Assessing the hazard. Nature 367, 33–40. https://doi.org/10.1038/367033a0

Coupe, J., Bardeen, C.G., Robock, A., Toon, O.B., 2019. Nuclear winter responses to nuclear war between the United States and Russia in the whole atmosphere community climate model version 4 and the Goddard Institute for Space Studies ModelE. J. Geophys. Res.

Atmospheres 124, 8522–8543. https://doi.org/10.1029/2019JD030509

DANVA, 2019. Drinking water companies in DANVA Statistics & Benchmarking [WWW Document]. URL https://www.e-pages.dk/danva/233/ (accessed 8.21.24).

Deng, S., Ma, S., Zhang, X., Zhang, S., 2020. Integrated detection of a complex underground water supply pipeline system in an old urban community in China. Sustainability 12, 1670. https://doi.org/10.3390/su12041670

Denkenberger, D., Pearce, J.M., 2018. Cost-effectiveness of interventions for alternate food in the United States to address agricultural catastrophes. Int. J. Disaster Risk Reduct. 27, 278–289. https://doi.org/10.1016/j.ijdrr.2017.10.014

Devoto, F., Duflo, E., Dupas, P., Parienté, W., Pons, V., 2012. Happiness on Tap: Piped Water Adoption in Urban Morocco. Am. Econ. J. Econ. Policy 4, 68–99. https://doi.org/10.1257/pol.4.4.68

Dijkstra, L., Hamilton, E., Lall, S., Wahba, S., 2020. How do we define cities, towns, and rural areas? [WWW Document]. World Bank Blogs. URL https://blogs.worldbank.org/en/sustainablecities/how-do-we-define-cities-towns-and-rural-areas (accessed 5.13.24).

Farewell, T.S., Hallett, S.H., Hannam, J.A., Jones, R.J.A., 2012. Soil impacts on national infrastructure in the UK [WWW Document]. URL https://www.itrc.org.uk/wp-content/PDFs/ITRC-Soil-impacts-on-NI-2013.pdf (accessed 12.11.24).

Federal State Statistics Service, 2019. Sustainable Development Goals in the Russian Federation: 2019 [WWW Document]. URL https://eng.rosstat.gov.ru/storage/mediabank/SDG_in_Russia_2019_ENG.pdf (accessed 10.5.24).

FEMA, 2024. Community Lifelines [WWW Document]. URL https://www.fema.gov/emergency-managers/practitioners/lifelines (accessed 12.12.24).

Forstall, R.L., Greene, R.P., Pick, J.B., 2009. Which are the largest? Why lists of major urban areas vary so greatly. https://doi.org/10.1111/j.1467-9663.2009.00537.x

Gia Pham, T., Kappas, M., Van Huynh, C., Hoang Khanh Nguyen, L., 2019. Application of ordinary kriging and regression kriging method for soil properties mapping in hilly region of Central Vietnam. ISPRS Int. J. Geo-Inf. 8, 147. https://doi.org/10.3390/ijgi8030147

Glazer, Y.R., Tremaine, D.M., Banner, J.L., Cook, M., Mace, R.E., Nielsen-Gammon, J., Grubert, E., Kramer, K., Stoner, A.M.K., Wyatt, B.M., Mayer, A., Beach, T., Correll, R., Webber, M.E., 2021. Winter Storm Uri: A test of Texas' water infrastructure and water resource resilience to extreme winter weather events. J. Extreme Events 08, 2150022. https://doi.org/10.1142/S2345737621500226

Gong, P., Li, X., Wang, J., Bai, Y., Chen, B., Hu, T., Liu, X., Xu, B., Yang, J., Zhang, W., Zhou, Y., 2020. Annual maps of global artificial impervious area (GAIA) between 1985 and 2018. Remote Sens. Environ. 236, 111510. https://doi.org/10.1016/j.rse.2019.111510

Google, 2024a. Google Maps - Bournemouth satellite imagery [WWW Document]. URL https://maps.app.goo.gl/LhnsKkY7qXpZ1s2g6 (accessed 12.21.24).

Google, 2024b. Google Maps - Valdosta satellite imagery [WWW Document]. URL https://maps.app.goo.gl/LDVvfQMSS1x1q1UR9 (accessed 12.21.24).

Google, 2024c. Google Maps - Nasirabad satellite imagery [WWW Document]. URL https://maps.app.goo.gl/FhGAwHCpJDizyzPt5 (accessed 12.21.24).

Grineski, S.E., Collins, T.W., Chakraborty, J., 2022. Cascading disasters and mental health inequities: Winter Storm Uri, COVID-19 and post-traumatic stress in Texas. Soc. Sci. Med. 315, 115523. https://doi.org/10.1016/j.socscimed.2022.115523

Haimes, Y.Y., Matalas, N.C., Lambert, J.H., Jackson, B.A., Fellows, J.F.R., 1998. Reducing vulnerability

of water supply systems to attack. J. Infrastruct. Syst. 4, 164–177.
https://doi.org/10.1061/(ASCE)1076-0342(1998)4:4(164)

Huang, X., Rudolph, D.L., Glass, B., 2022. A coupled thermal-hydraulic-mechanical approach to modeling the impact of roadbed frost loading on water main failure. Water Resour. Res. 58, e2021WR030933. https://doi.org/10.1029/2021WR030933

Instituto Brasileiro de Geografia e Estatística, n.d. Cidades e Estados: São Paulo: Código: 3550308 [WWW Document]. URL https://www.ibge.gov.br/cidades-e-estados/sp/sao-paulo.html (accessed 2.16.24).

Irish Water, 2015. Water services strategic plan: A plan for the future of water services [WWW Document]. URL https://www.water.ie/sites/default/files/docs/WSSP_Final.pdf (accessed 8.21.24).

Jeffay, J., 2022. Satellites spot leaking water pipes from way above Earth. NoCamels. URL https://nocamels.com/2022/10/satellites-spot-leaking-water-pipes-from-way-above-earth/ (accessed 10.24.24).

Jehn, F.U., Gajewski, Ł.G., Hedlund, J., Arnscheidt, C.W., Xia, L., Wunderling, N., Denkenberger, D., 2024. Food trade disruption after global catastrophes. https://doi.org/10.31223/X5MQ4R

Jones, E.R., van Vliet, M.T.H., Qadir, M., Bierkens, M.F.P., 2021. Country-level and gridded estimates of wastewater production, collection, treatment and reuse. Earth Syst. Sci. Data 13, 237–254. https://doi.org/10.5194/essd-13-237-2021

Jordan, L., Watkins, B., Biegon, P., Mwangi, M., Rose, R., 2010. Practical approaches to spatial estimation of disaster-affected populations. Int. J. Appl. Geospatial Res. 1, 31–48. https://doi.org/10.4018/jagr.2010070103

Kadri, F., Birregah, B., Châtelet, E., 2014. The impact of natural disasters on critical infrastructures: A domino effect-based study. J. Homel. Secur. Emerg. Manag. 11, 217–241. https://doi.org/10.1515/jhsem-2012-0077

Karamouz, M., Saadati, S., Ahmadi, A., 2012. Vulnerability assessment and risk reduction of water supply systems. World Environ. Water Resour. Congr. 2010 Chall. Change 4414–4426. https://doi.org/10.1061/41114(371)449

Lebakula, V., Epting, J., Moehl, J., Stipek, C., Adams, D., Reith, A., Kaufman, J., Gonzales, J., Reynolds, B., Basford, S., Martin, A., Buck, W., Faxon, A., Cunningham, A., Roy, A., Barbose, Z., Massaro, J., Walters, S., Woody, C., Iman, A., Wilkins, A., Powell, E., Urban, M., 2024. LandScan Silver Edition. https://doi.org/10.48690/1531770

LeChevallier, M.W., Gullick, R.W., Karim, M.R., Friedman, M., Funk, J.E., 2003. The potential for health risks from intrusion of contaminants into the distribution system from pressure transients. J. Water Health 1, 3–14. https://doi.org/10.2166/wh.2003.0002

Macao Water, 2018. 2018 annual report: Embracing green future with smart water [WWW Document]. URL https://www.macaowater.com/sites/default/files/report/annals/2018_Annual%20report%20 2.pdf (accessed 7.23.24).

Mair, M., Zischg, J., Rauch, W., Sitzenfrei, R., 2017. Where to find water pipes and sewers?—On the correlation of infrastructure networks in the urban environment. Water 9, 146. https://doi.org/10.3390/w9020146

Mayny, S.B., Chernikov, N.A., Tvardovskaya, N.V., 2024. Experience in construction and operation of sewerage networks in areas with deep seasonal ground freezing across different regions of the Russian Federation. E3S Web Conf. 549, 03006. https://doi.org/10.1051/e3sconf/202454903006

Meehan, K., Jurjevich, J.R., Chun, N.M.J.W., Sherrill, J., 2020. Geographies of insecure water access and the housing–water nexus in US cities. Proc. Natl. Acad. Sci. 117, 28700–28707.

https://doi.org/10.1073/pnas.2007361117

Melaku, N.D., Fares, A., Awal, R., 2023. Exploring the impact of winter storm Uri on power outage, air quality, and water systems in Texas, USA. Sustainability 15, 4173. https://doi.org/10.3390/su15054173

Milman, A., Kumpel, E., Lane, K., 2021. The future of piped water. Water Int. 46, 1000–1016. https://doi.org/10.1080/02508060.2021.1995169

Moriconi-Ebrard, F., 1991. [The 100 largest cities in the world]. Econ. Stat.

NASA, 2017. S3001: Guidelines for risk management [WWW Document]. URL https://www.nasa.gov/wp-content/uploads/2015/10/s3001_guidelines_for_risk_management_-_ver_g_-_10-25-2017.pdf (accessed 1.31.24).

National Bureau of Statistics of China, 2019. China Statistical Yearbook 2019 [WWW Document]. URL https://www.stats.gov.cn/sj/ndsj/2019/html/E2505.jpg (accessed 1.11.25).

OECD, 2024. Indicators: Indicator: Density of road (km per one hundred sq. km) [WWW Document]. URL https://data-explorer.oecd.org/vis?tenant=archive&df%5Bds%5D=DisseminateArchiveDMZ&df%5Bid%5D=DF_ITF_INDICATORS&df%5Bag%5D=OECD&dq=.IND-INFR-ROAD-DENS&lom=LASTNPERIODS&lo=5&to%5BTIME_PERIOD%5D=false&vw=tb&ly%5Bcl%5D=TIME_PERIOD&ly%5Brw%5D=COUNTRY (accessed 12.20.24).

Oladunmoye, O., 2024. Rapid urbanization and the Nigerian landscape: The gains, the menaces, and strategies for future success. Soc. Inform. J. 3, 39–44. https://doi.org/10.58898/sij.v3i1.39-44

OpenStreetMap contributors, 2024. Highways - OpenStreetMap Wiki [WWW Document]. URL https://wiki.openstreetmap.org/wiki/Highways (accessed 11.12.24).

Ouyang, W., Shan, Y., Hao, F., Chen, S., Pu, X., Wang, M.K., 2013. The effect on soil nutrients resulting from land use transformations in a freeze-thaw agricultural ecosystem. Soil Tillage Res. 132, 30–38. https://doi.org/10.1016/j.still.2013.04.007

Pauliuk, S., Venkatesh, G., Brattebø, H., Müller, D.B., 2014. Exploring urban mines: Pipe length and material stocks in urban water and wastewater networks. Urban Water J. 11, 274–283. https://doi.org/10.1080/1573062X.2013.795234

Pericault, Y., Risberg, M., Vesterlund, M., Viklander, M., Hedström, A., 2017. A novel freeze protection strategy for shallow buried sewer pipes: Temperature modelling and field investigation. Water Sci. Technol. 76, 294–301. https://doi.org/10.2166/wst.2017.174

Pirestani, N., Ahmadi Nadoushan, M., Abolhasani, M.H., Zamani Ahmadmahmoudi, R., 2024. Mapping soil characteristics: Spatio-temporal comparison of land use regression and ordinary kriging in an arid environment. J. Indian Soc. Remote Sens. https://doi.org/10.1007/s12524-023-01804-y

Pozzi, F., Small, C., 2002. Vegetation and population density in urban and suburban areas in the U.S.A., in: Makiav, D., Jürgens, C., Sunar-Erbek, F., Akguen, H. (Eds.), Proceedings. Presented at the 3rd International Symposium on Remote Sensing of Urban Areas, Istanbul, Turkey 11–13 June, Istanbul Technical University, Istanbul, pp. 489–496.

Rajani, B., Kleiner, Y., 2001. Comprehensive review of structural deterioration of water mains: Physically based models. Urban Water, Ground Water in the Environment 3, 151–164. https://doi.org/10.1016/S1462-0758(01)00032-2

Republic of Lebanon Ministry of Energy and Water, 2020. National water sector strategy update - 2020: Volume II: Water sector governance [WWW Document]. URL https://faolex.fao.org/docs/pdf/leb211916EVolII.pdf (accessed 7.15.24).

Rezaei, H., Ryan, B., Stoianov, I., 2015. Pipe failure analysis and impact of dynamic hydraulic conditions in water supply networks. Procedia Eng., Computing and Control for the Water Industry (CCWI2015) Sharing the best practice in water management 119, 253–262.

https://doi.org/10.1016/j.proeng.2015.08.883

Robock, A., Oman, L., Stenchikov, G.L., 2007. Nuclear winter revisited with a modern climate model and current nuclear arsenals: Still catastrophic consequences. J. Geophys. Res. Atmospheres 112. https://doi.org/10.1029/2006JD008235

Romanovsky, V., Burgess, M., Smith, S., Yoshikawa, K., Brown, J., 2002. Permafrost temperature records: Indicators of climate change. Eos Trans. Am. Geophys. Union 83, 589–594. https://doi.org/10.1029/2002EO000402

Rose, A.N., Bright, E.A., 2014. The LandScan Global population distribution project: Current state of the art and prospective innovation [WWW Document]. URL https://web.archive.org/web/20220617085723/https://paa2014.princeton.edu/papers/143242 (accessed 1.3.25).

Rougier, J., Sparks, R.S.J., Cashman, K.V., Brown, S.K., 2018. The global magnitude–frequency relationship for large explosive volcanic eruptions. Earth Planet. Sci. Lett. 482, 621–629. https://doi.org/10.1016/j.epsl.2017.11.015

Sargaonkar, A., Nema, S., Gupta, A., Sengupta, A., 2010. Risk assessment study for water supply network using GIS. J. Water Supply Res. Technol.-Aqua 59, 355–360. https://doi.org/10.2166/aqua.2010.090

Selezneva, O.I., Jiang, Y.J., Larson, G., Puzin, T., 2008. Long-term pavement performance computed parameter: Frost penetration [WWW Document]. URL https://www.fhwa.dot.gov/publications/research/infrastructure/pavements/ltpp/08057/080 57.pdf (accessed 12.5.24).

Stantec, n.d. PipeWATCH™: Maintain the safety and integrity of your pipeline infrastructure [WWW Document]. Stantec.io. URL https://www.stantec.com/en/services/digital/pipewatch (accessed 10.24.24).

Statistical Committee of the Republic of Armenia, n.d. Water supply system of the Republic by indicators, marzes and years [WWW Document]. URL https://statbank.armstat.am/pxweb/en/ArmStatBank/ArmStatBank__2%20Population%20a nd%20social%20processes__26%20Housing__263%20Jrmux/PS-hs-ws01.px/table/tableVie wLayout2/?rxid=9ba7b0d1-2ff8-40fa-a309-fae01ea885bb (accessed 7.26.24).

Szpak, D., Szczepanek, A., 2023. A new method of water supply in crisis situation. Water 15, 3160. https://doi.org/10.3390/w15173160

Taubenböck, H., Weigand, M., Esch, T., Staab, J., Wurm, M., Mast, J., Dech, S., 2019. A new ranking of the world's largest cities—Do administrative units obscure morphological realities? Remote Sens. Environ. 232, 111353. https://doi.org/10.1016/j.rse.2019.111353

Toon, O.B., Robock, A., Turco, R.P., 2008. Environmental consequences of nuclear war. Phys. Today 61, 37–42. https://doi.org/10.1063/1.3047679

Turco, R.P., Toon, O.B., Ackerman, T.P., Pollack, J.B., Sagan, C., 1983. Nuclear winter: Global consequences of multiple nuclear explosions. Science 222, 1283–1292. https://doi.org/10.1126/science.222.4630.1283

United Nations, 2022. Human Development Index [WWW Document]. Hum. Dev. Rep. URL https://hdr.undp.org/data-center/human-development-index (accessed 12.19.24).

United Nations, Department of Economic and Social Affairs, Population Division, 2019. World Urbanization Prospects: The 2018 revision (ST/ESA/SER.A/420) [WWW Document]. URL https://population.un.org/wup/assets/WUP2018-Report.pdf (accessed 1.4.25).

United Nations General Assembly, 2017. Resolution adopted by the General Assembly on 6 July 2017: Work of the Statistical Commission pertaining to the 2030 Agenda for Sustainable Development.

United Nations General Assembly, 2015. Resolution adopted by the General Assembly on 25

September 2015: Transforming our world: The 2030 Agenda for Sustainable Development.

United Nations Statistical Commission, 2024. Global indicator framework for the Sustainable Development Goals and targets of the 2030 Agenda for Sustainable Development.

United Nations Statistics Division, n.d. SDG indicators [WWW Document]. Sustain. Dev. Goals. URL https://unstats.un.org/sdgs/indicators/indicators-list/ (accessed 11.13.24).

US Census Bureau, 2024. Current population [WWW Document]. URL https://www.census.gov/popclock/print.php?component=counter (accessed 12.19.24).

U.S. Environmental Protection Agency, 2018. Drinking water infrastructure needs survey and assessment: Sixth report to Congress [WWW Document]. URL https://www.epa.gov/sites/production/files/2018-10/documents/corrected_sixth_drinking_water_infrastructure_needs_survey_and_assessment.pdf (accessed 10.4.24).

Van Leuven, L.J., 2011. Water/wastewater infrastructure security: Threats and vulnerabilities, in: Clark, R.M., Hakim, S., Ostfeld, A. (Eds.), Handbook of Water and Wastewater Systems Protection, Protecting Critical Infrastructure. Springer, New York, NY, pp. 27–46. https://doi.org/10.1007/978-1-4614-0189-6_2

van Thienen, P., Chatzistefanou, G.A., Makropoulos, C., Vamvakeridou-Lyroudia, L., 2023. What water supply system research is needed in the face of a conceivable societal collapse? J. Water Clim. Change 14, 4635–4641. https://doi.org/10.2166/wcc.2023.351

VKR - Verband Kunststoff-Rohre und -Rohrleitungsteile, Possamai, M., Niederer, U., Weber, H., Baumgartner, P., 2019. Anbohren von PE-Rohren [WWW Document]. URL http://brunnenmeister.ch/assets/pdf/658565e02a3aa.pdf (accessed 9.11.24).

Water UK, 2022. A leakage routemap to 2050 [WWW Document]. URL https://www.water.org.uk/wp-content/uploads/2022/03/Water_UK_A-LEAKAGE-ROUTEMAP-TO-2050_Low-Res_V3.pdf (accessed 11.13.24).

Watson, K., Cross, R., Jones, M., Buttorff, G., Pinto, P., Sipole, S., Vallejo, A., 2021. The winter storm of 2021 [WWW Document]. URL https://uh.edu/hobby/winter2021/storm.pdf (accessed 8.31.21).

Wéber, R., Huzsvár, T., Hős, C., 2020. Vulnerability analysis of water distribution networks to accidental pipe burst. Water Res. 184, 116178. https://doi.org/10.1016/j.watres.2020.116178

WHO, UNICEF, 2023. Joint Monitoring Programme for Water Supply, Sanitation and Hygiene: Estimates for drinking water, sanitation and hygiene services by country (2000-2022): National data for menstrual health by country (2009-2022): Countries, areas and territories [WWW Document]. URL https://washdata.org/data/country/WLD/household/download (accessed 12.19.24).

WHO, UNICEF, 2021. SDG indicator metadata: (Harmonized metadata template - format version 1.0) [WWW Document]. URL https://washdata.org/report/jmp-2021-metadata-sdg-611 (accessed 12.12.24).

WHO, UNICEF, n.d. Trends in drinking water service levels, 2000-2022 [WWW Document]. URL https://washdata.org/data/household#!/dashboard/6386 (accessed 12.11.24).

Winter, J.C., Darmstadt, G.L., Davis, J., 2021. The role of piped water supplies in advancing health, economic development, and gender equality in rural communities. Soc. Sci. Med. 270, 113599. https://doi.org/10.1016/j.socscimed.2020.113599

Wolf, J., Johnston, R.B., Ambelu, A., Arnold, B.F., Bain, R., Brauer, M., Brown, J., Caruso, B.A., Clasen, T., Colford, J.M., Mills, J.E., Evans, B., Freeman, M.C., Gordon, B., Kang, G., Lanata, C.F., Medlicott, K.O., Prüss-Ustün, A., Troeger, C., Boisson, S., Cumming, O., 2023. Burden of disease attributable to unsafe drinking water, sanitation, and hygiene in domestic settings: A global analysis for selected adverse health outcomes. Lancet Lond. Engl. 401, 2060–2071. https://doi.org/10.1016/S0140-6736(23)00458-0

Wols, B.A., Thienen, P. van, 2016. Impact of climate on pipe failure: Predictions of failures for

drinking water distribution systems. Eur. J. Transp. Infrastruct. Res. 16.
https://doi.org/10.18757/ejtir.2016.16.1.3123

World Bank, 2024a. World Bank Country and lending groups [WWW Document]. World Bank Data
Help Desk. URL
https://datahelpdesk.worldbank.org/knowledgebase/articles/906519-world-bank-country-a
nd-lending-groups (accessed 10.29.24).

World Bank, 2024b. GDP (current US$) (NY.GDP.MKTP.CD) [WWW Document]. URL
https://databank.worldbank.org/reports.aspx?source=2&series=NY.GDP.MKTP.CD&country
(accessed 12.18.24).

World Bank, 2024c. Health Nutrition and Population Statistics: Population estimates and
projections [WWW Document]. URL
https://databank.worldbank.org/source/population-estimates-and-projections (accessed
12.18.24).

World Bank, 2021. Nigeria: Ensuring water, sanitation and hygiene for all [WWW Document]. World
Bank. URL
https://www.worldbank.org/en/news/feature/2021/05/26/nigeria-ensuring-water-sanitation
-and-hygiene-for-all (accessed 2.17.24).

Xia, L., Robock, A., Scherrer, K., Harrison, C.S., Bodirsky, B.L., Weindl, I., Jägermeyr, J., Bardeen, C.G.,
Toon, O.B., Heneghan, R., 2022. Global food insecurity and famine from reduced crop,
marine fishery and livestock production due to climate disruption from nuclear war soot
injection. Nat. Food 3, 586–596. https://doi.org/10.1038/s43016-022-00573-0

Xuecao, L., Gong, P., Zhou, Y., Wang, J., Bai, Y., Chen, B., Ty, H., Xiao, Y., Xu, B., Yang, J., Liu, X., Cai, W.,
Huang, H., Wu, T., Wang, X., Lin, P., Li, X., Chen, J., He, C., Zhu, Z., 2020. Mapping global
urban boundaries from the global artificial impervious area (GAIA) data. Environ. Res. Lett.
15. https://doi.org/10.1088/1748-9326/ab9be3

Zhang, T., Barry, R., 2006. Arctic EASE-Grid freeze and thaw depths, 1901 - 2002, version 1.
https://doi.org/10.7265/B3PG-BK18

Zhao, M., Cheng, C., Zhou, Y., Li, X., Shen, S., Song, C., 2022. A global dataset of annual urban extents
(1992–2020) from harmonized nighttime lights. Earth Syst. Sci. Data 14, 517–534.
https://doi.org/10.5194/essd-14-517-2022

Zhao, N., Tilottama, G., Currit, N., Elvidge, C., 2011. Relationships between satellite observed lit area
and water footprints. Water Resour. Manag. 25, 2241–2250.
https://doi.org/10.1007/s11269-011-9804-3

Zhu, Q., Lin, H.S., 2010. Comparing ordinary kriging and regression kriging for soil properties in
contrasting landscapes. Pedosphere 20, 594–606.
https://doi.org/10.1016/S1002-0160(10)60049-5

Zohra, H.F., Mahmouda, B., Luc, D., 2012. Vulnerability assessment of water supply network. Energy
Procedia, Terragreen 2012: Clean Energy Solutions for Sustainable Environment (CESSE)
18, 772–783. https://doi.org/10.1016/j.egypro.2012.05.093

Żywiec, J., Szpak, D., Wartalska, K., Grzegorzek, M., 2024. The impact of climate change on the
failure of water supply infrastructure: A bibliometric analysis of the current state of
knowledge. Water 16, 1043. https://doi.org/10.3390/w16071043

Росстат, 2022. Водопровод в России [WWW Document]. VK. URL
https://vk.com/wall-152641130_6740 (accessed 12.20.24).